Biomedicine & Pharmacotherapy 149 (2022) 112883

Contents lists available at ScienceDirect

Biomedicine & Pharmacotherapy

journal homepage: www.elsevier.com/locate/biopha

In vivo antitumor activity of *Euphorbia lathyris* ethanol extract in colon cancer models

C. Mesas [a,b,c], R. Martínez [d,e], K. Doello [f], R. Ortiz [a,b,c], M. López-Jurado [e], Francisco Bermúdez [d], F. Quiñonero [a,b], J. Prados [a,b,c,*], J.M. Porres [e], C. Melguizo [a,b,c]

[a] Institute of Biopathology and Regenerative Medicine (IBIMER), Center of Biomedical Research (CIBM), University of Granada, 18100 Granada, Spain
[b] Department of Anatomy and Embryology, Faculty of Medicine, University of Granada, 18071 Granada, Spain
[c] Instituto de Investigación Biosanitaria de Granada (ibs.GRANADA), 18014 Granada, Spain
[d] Cellbitec S.L., N.I.F. B04847216, Scientific Headquarters of the Almería Technology Park, Universidad de Almería, 04128 La Cañada, Almería, Spain
[e] Department of Physiology, Institute of Nutrition and Food Technology (INyTA), Center of Biomedical Research (CIBM), University of Granada, 18100 Granada, Spain
[f] Medical Oncology Service, Virgen de las Nieves Hospital, 18014 Granada, Spain

ARTICLE INFO

Keywords:
Colon cancer
Euphorbia lathyris
AOM/DSS model
Orthotopic xenograft model
Oxidative stress detoxification enzymes
Microbiome

ABSTRACT

Euphorbia lathyris seeds have been used to treat various medical conditions. We previously reported that ethanolic extract from the defatted seed of Euphorbia lathyris (EE) (variety S3201) possesses a potent *in vitro* antitumor activity against colon cancer (CRC) cell lines. However, the effects of EE on CRC *in vivo* models and its possible preventive activity have not been elucidated. The aim of this study is to develop an *in vivo* study to corroborate its efficacy. For this purpose, two tumor induction models have been developed. In orthotopic xenograft model, it has been shown that EE reduces tumor size without hematological toxicity. The ethanolic extract induced an intense apoptosis in tumors mediated by caspase 3. Using the Azoxymethane/Dextran Sulfate Sodium model, a reduction of dysplastic polyps has been demonstrated, showing its preventive power. Furthermore, EE promoted the presence of an eubiotic microbiotal environment in the mucosa of the colon and induced an increase in antioxidant enzyme activity. This fact was accompanied by a modulation of cytokine expression that could be related to its protective mechanism. Therefore, although further experiments will be necessary to determine its applicability in the treatment of CRC, ES could be a new prevention strategy as well as treatment for this type of tumor, being a powerful candidate for future clinical trials.

1. Introduction

Colorectal cancer (CRC) currently ranks the third most common type of cancer worldwide in both sexes and the second cause of cancer-related mortality, causing up to 1 million deaths annually [1,2]. Dietary patterns and lifestyle, including physical inactivity, excess body weight, red and processed meats and refined carbohydrates, chronic hyperinsulinemia, alcohol consumption, and early smoking are modifiable and preventable risk factors for CRC [3]. In addition, the development of screening programs (secondary prevention) for early detection of CRC, offers the opportunity to detect premalignant lesions [4]. However, despite prevention measures, the incidence of CRC remains high, both at non-metastatic stages —usually treated with surgical resection [5]— an advanced stages —which require chemotherapy treatment (*e.g.*, 5-Fluorouracil, Capecitabine, Irinotecan, or Oxaliplatin, administered alone or in combination) [6,7]. Moreover, monoclonal antibodies and multiple kinase inhibitors are being used to improve patient prognosis [8]. Remarkably, 20–25% of patients present with metastatic CRC at disease onset, and 50% of patients will eventually develop metastases [9]. In these cases, currently available therapies have not achieved significant modifications in the 5-year overall survival rates, which remain below 15% [10]. Furthermore, chemotherapeutic drugs cause adverse effects and drug resistance, which decrease life expectancy and quality [11]. Therefore, the development of new therapeutic alternatives that improve the results of current treatments is a priority [12].

In this context, plant extracts as a source of antitumor bioactive compounds are gaining great importance, being considered a new

* Corresponding author at: Institute of Biopathology and Regenerative Medicine (IBIMER), Center of Biomedical Research (CIBM), University of Granada, 18100 Granada, Spain.
E-mail address: jcprados@ugr.es (J. Prados).

https://doi.org/10.1016/j.biopha.2022.112883
Received 28 January 2022; Received in revised form 9 March 2022; Accepted 23 March 2022
Available online 5 April 2022

therapeutic strategy [13,14]. Specifically, the genus *Euphorbia*, belonging to the *Euphorbiaceae* family, has shown significant antioxidant, anti-inflammatory, hepatoprotective and antitumor effects [15]. Recently, we used *Euphorbia lathyris* seeds (variety S3201) to develop an ethanolic extract (*Euphorbia lathyris* ethanolic extract-EE) with a high proportion of polyphenols, including esculetin, euphorbetin, gaultherin and kaempferol-3-rutinoside [16]. Previous studies showed that similar seeds contained numerous diterpenes and triterpenes [17], lathyran-type diterpenoids [18], and ingenol and Euphorbia factors [19], among other biologically active compounds. Recently, some of these compounds exhibited antitumor activity against leukemia, skin cancer [20,21] and hepatocellular carcinoma [22], and even ability to modulate chemotherapy resistance mechanisms (*e.g.*, P-glycoprotein) [23]. Our *in vitro* assays demonstrated striking antitumor activity against colon cancer cells (both resistant and non-resistant) through activation of apoptosis and autophagy. Interestingly, the EE also showed great activity against colon cancer stem cells (CSCs), suggesting its potential use as a new therapeutic strategy for the treatment of CRC [16].

Finally, recent studies associated the high presence of polyphenol content in fruits and seeds with benefits on gut microbiota [24]. Modulation of the microbiota seems an essential process in colon cancer initiation, progression and resistance [25]. In fact, there are numerous changes in the microbiome associated with different tumor stages [26]. Some studies demonstrated antitumor effects and ability to promote the regulation of the microbiota in different plant extracts. A probiotic consisting of lactobacillus gasseri 505 and *Cudrarnia tricuspidata* leaf extract in fermented milk (FCT) showed a protective effect against colon cancer in an *in vivo* model of Azoxymethane (AOM)/Dextran Sulfate Sodium (DSS) administration by regulating inflammation, carcinogenesis and modulation of the intestinal microbiota by increasing the population of *Lactobacillus*, *Bifidobacterium* and *Akkermansia* [27]. Likewise, different polyphenols and their metabolites showed ability to induce changes in the microbiota which protect against mucosal alterations such as colitis and even CRC [28].

The aim of this study was to corroborate the *in vivo* antitumor activity of the *E. lathyris* EE, which already demonstrated significant antiproliferative activity on different colon cancer cell lines. To evaluate this antitumor effect, two different models of colon cancer were used, a heterotopic xenograft model obtained by subcutaneous implantation of tumor cells, and a model of colon carcinogenesis induced by AOM/DSS. Our results suggest that our ethanolic extract of *E. lathyris* may be a new therapeutic strategy to improve CRC treatment.

2. Materials and methods

2.1. Plant Material and ethanolic extract development

Mature seeds of *E. lathyryis* (variety S3201) were transferred by Agrointec Solutions S.L. (Almería, Spain). The ethanolic extract, after a seed defatting process carried out by CELLBITEC S.L, was developed following our own protocol [16]. Briefly, an ethanolic extract (Ethanol: type I water: 12 N HCl; 50:50:0.2) was obtained by two serial extractions (pH 2, and temperature 4 °C in a reducing atmosphere for 30 min in a magnetic stirrer). Once the ethanolic extract was obtained, the ethanol was evaporated using a vacuum evaporator (Savant DNA120 SpeedVac Concentrator, ThermoSci, Waltham, MA, USA) (Eppendorf Concentrator 5301). Finally, the ethanolic extract from defatted seeds of *E. lathyris* was resuspended in saline serum to a concentration of 25 mg/mL, aliquoted and stored at − 20 °C until administration.

2.2. Hemolysis assay

The hemolysis assay was performed using human blood from a healthy donor (25 mL in collection tubes with EDTA) (Andalusian Public Health System Biobank) and following our own protocol [29]. After erythrocyte dilution (1:50) (pH 7.4), 190 μl was added to 96-well plates. Similarly, EE was added at different concentrations (1–100 ug/mL) in a volume of 10 μl per well. Triton X-100 (10 μl; 20%) and phosphate buffer pH 7.4 (10 μl) were used as positive and negative controls, respectively. The plate was incubated for 1 h at 37 °C with shaking (15 rpm), centrifuged at 500xg for 5′, and the supernatant (100 μl) was transferred to another 96-well plate. The percentage of hemoglobin released by erythrocytes was determined by spectrophotometry (wavelength of 492 nm) with a Titertekmultiscan colorimeter (492 nm) (Flow, Irvine, California) using the formula:

$$Hemolysis(\%) = \frac{abs.of\ the\ sample - abs.of\ the\ negative\ control}{abs.of\ the\ positive\ control} x100$$

To analyze morphological modifications, light microscopy images of erythrocytes exposed to EE were taken.

2.3. Peripheral lymphocyte assay

White blood cells (WBCs) from healthy donors (25 mL of blood) were isolated using Ficoll-Paque (v/v) to perform a proliferation assay following our own protocol [30]. The cells were cultured in 96-well plates (2×10^4 cells/well) in a volume of 90 μl. EE (10 μl) was added to each well from a stock solution to reach a final concentration ranging from 1 to 100 μg/mL and were incubated for 1 and 12 h at 37 °C and 5% CO2 in a humidified atmosphere. Then, the viability of WBCs was determined by the Cell Counting Kit-8 (CCK-8) (Sigma-Aldrich, Saint Louis, MO, USA) after an incubation (3 h) with CCK-8 solution (10%). Absorbance at 450 nm was measured using a microplate reader.

2.4. In vivo assays

Brown female C57BL/6 mice (weight 18–20 g, 6 weeks old) (Charles River Laboratories Inc, Wilmington, MA, USA) were used in all *in vivo* experiments. Mice were housed in colony cages with free access to water and food prior to the experiments. The light and temperature were always controlled (22 °C, and 12 h light–dark cycle). All animal studies were approved by the Ethics Committee on Animal Experimentation of the University of Granada (Reference code: 16/01/2020/005) and in accordance with international standards (European Communities Council Directive 2010/63).

2.4.1. Orthotopic xenograft murine colorectal cancer models

For subcutaneous tumor induction, the MC-38 murine CRC cell line (American Type Culture Collection, Rockville, MD, USA) was cultured *in vitro* with Dulbecco's Modified Eagle's Medium (DMEM) (Sigma-Aldrich, Madrid, Spain) supplemented with 10% fetal bovine serum (FBS) (Gibco, Madrid, Spain) and 1% antibiotic composed by streptomycin and amphotericin B mixture (ATB) (Sigma Aldrich, Madrid, Spain). Subcutaneous tumors were induced injecting 5×10^5 cells of the MC38 cell line resuspended in 100 μl of PBS into the right flank of the animal. When tumors were palpable (2 × 2 mm), mice were randomly divided into 2 groups (n = 14): a control group (CT+) and a group treated with EE. Treatment with EE (250 mg/Kg) was administered by intraperitoneal injection every 3 days for a total of 7 doses of EE. The weight of the animal was controlled, tumor growth was monitored by measuring its dimensions with a digital capillary every 3 days. Tumor volume (mm^3) was calculated using the following formula:

$$V \quad (mm^3) = \frac{a \quad x \quad b^2 \quad x \quad \pi}{6}$$

where "a" is the largest diameter of the tumor, and "b" is the largest diameter perpendicular to "a". The end point of the experiment and the sacrifice of mice was day 40 from the inoculation of tumor cells. Finally, samples from tumor and different organs (liver, lung and spleen) were obtained for inclusion in paraformaldehyde (Fig. 1A).

2.4.2. AOM/DSS induction of colorectal cancer model

A total of 28 mice were treated with a single intraperitoneal injection

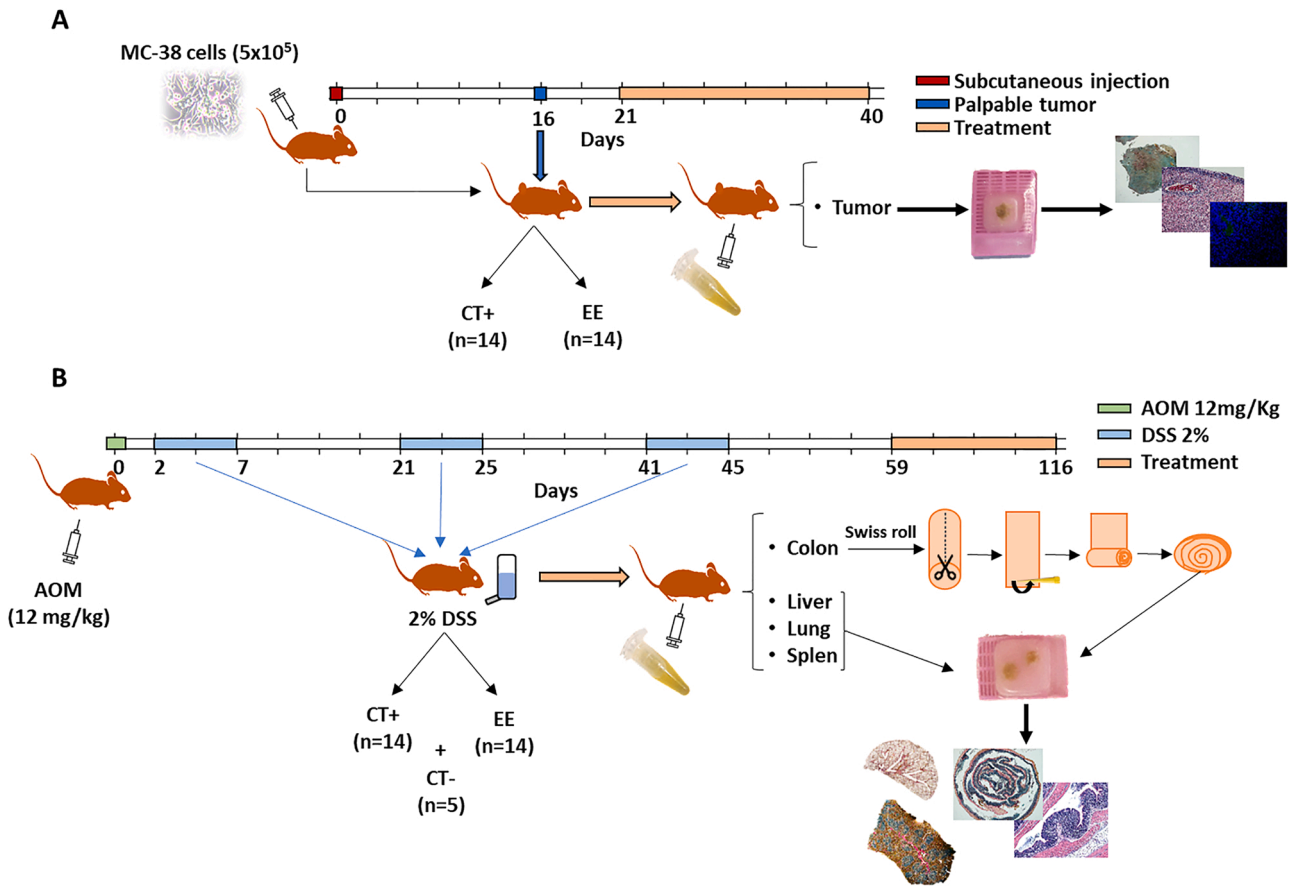

Fig. 1. Schematic representation of the *in vivo* assay using two CRC induction models. A) Orthotopic xenograft murine CRC cancer model. After 16 days of cell inoculation, a subcutaneous tumor was detected. Treatment with EE was applied during 19 days using an intraperitoneal injection every 3 days. After mice sacrifice, tumor samples were obtained for histological analysis. B) AOM/DSS induction of CRC cancer model. Tumor induction was developed during 59 days. Treatment with EE was applied during 57 days using an intraperitoneal injection every 3 days. After mice sacrifice, organs were obtained for histological analysis. In addition, the Swiss-roll technique was carried out to preserve the colon and to perform histological analysis.

of AOM (12 mg/kg) (Sigma-Aldrich, Madrid, Spain). After 48 h, mice received 2% DSS (Sigma-Aldrich) in drinking water for 5 days. After a 15-day rest period with normal water, a second cycle of 2% DSS was administered for 5 days and, subsequently, a 5-day cycle of 3% DSS. After the last 15 days of rest, mice were randomly allocated into two groups (n = 14): a group control (CT+) and a group treated with EE. In addition, a third group (n = 5) was formed with healthy mice (CT-). Treatment (250 mg/Kg) was administered by intraperitoneal injection every 3 days for a total of 19 doses. During the 57 days of treatment, the CT+ and CT- groups had free access to water and food. The end point of the experiment and the sacrificed of mice was on the 116th day from injection of AOM. Samples of different organs (liver, lung and spleen) were preserved for subsequent fixation in paraformaldehyde. In this case, colon samples were included using the Swiss-rolling technique [31] (Fig. 1B).

2.5. Morphological and histological analysis: polyps size and distribution

The colon of mice was obtained by incision, opened and photographed using ImageJ to count and measure polyps. Samples from tumor, organs and Swiss-roll were fixed in paraformaldehyde (24 h) and included in paraffin blocks to obtain 5 μm sections with a rotary microtome (Leica, Wetzlar, Germany). After deparaffinizing and hydrating, the sections were stained with hematoxylin-eosin (H&E) and pentachrome methods [32]. In addition, caspase 3 (sc-271759) expression was analyzed using immunofluorescence (mAbs at 1:100). Alexa-488® was used as secondary mAb (sc-2359, Santa Cruz Biotechnology, INC.) These images were obtained with a photographic microscope (Nikkon Eclipse Ni, Melville, USA).

2.6. Carbonic anhydrase analysis in tumor

To determine the carbonic anhydrase activity of cancer tissue, samples from subcutaneous tumors were conserved in liquid nitrogen, homogenized and processed following the protocol described by Gai et al. [33]. Briefly, cold carbonated water was added to the homogenized samples (2 μg of total protein) and phenol red was used as a colorimetric pH marker. Absorbance at 557 nm was measured using a spectrophotometer (Titertekmultiscan colorimeter, Flow, Irvine, California).

2.7. Hematological toxicity analysis

To evaluate the possible hemotoxicity of EE, analysis of mice blood was carried out. Before euthanasia, mice were anesthetized and a blood sample (1 mL/animal) was collected by cardiac puncture. The hemogram was processed in Mslab21 Medical Lab Fully Auto Hematology Analyzer/Cbc Test Machine (Medsinglong Global Group Co, China).

2.8. DNA extraction and bacterial identification in cecal samples

After mice were euthanized, colon contents were collected for microbiota profiling. Cecal content collected at the end of the experiment was used for genomic DNA (gDNA) isolation. Extraction was carried out using the QIAamp® PowerFecal® DNA kit following the

manufacturer's protocol for process automation with the QIAcube robot. Quantification of gDNA was performed by fluorometry (qubit). gDNA samples were analyzed by sequencing the V4 region (233 bp) of 16S ribosomal RNA (rRNA) genes using the MiSeq system (Illumina, San Diego, CA, USA). Library preparation, pooling, and miniSeq sequencing were performed at the Institute of Parasitology and Biomedicine "López-Neyra" (IPBLN) from the Spanish National Research Council (CSIC). Reaction steps were as follows: denaturation 3 min at 95 °C, (denaturation 30 s at 95 °C, annealing 30 s at 55 °C, elongation 30 s at 72 °C) × 25 cycles, and extension 5 min at 72 °C indexed with 8 PCR cycles to amplify the V3-V4 regions of the 16S rRNA gene with the following primers: 16 S ProV3V4 forward 5′->3′ 5′ CCTACGGGNBGCASCAG 3′ and 16S ProV3V4 reverse 5′->3′ 5′ GACTACNVGGGTATCTAATCC 3′. Results were obtained from the Illumina analysis software version 2.6.2.3 and presented for the taxonomic levels of Phylum, Family and Genus according to the top 8 or 9 for each taxonomic level.

2.9. RNA extraction and quantitative RT-PCR of colon gene expression

Total RNA was isolated from a portion of colon by homogenization in 1 mL of Tri-Reagent (Sigma-Aldrich). RNA was solubilized in Rnase-free H_2O and treated with DNase (Applied Biosystems) to remove any DNA present in the sample. A total of 100–250 ng of RNA was reverse-transcribed according to standard protocols using a Lifepro Thermal Cycler (Bioer Serves Life, China). Quantitative RT-PCR was performed with QuantStudio 12 K Flex Real-Time PCR System (Applied Biosystems) using primer/probes for genes involved in oxidative metabolism (Nfe2l2, sod1, sod2, cat, gpx2), genes coding for detoxification pathways (NQO1 and gsta2), markers involved in inflammatory processes (Tnf, IL-1b y IL-6) and glucose metabolism (gcg) (Applied Biosystems). The PCR master mix reaction included the first-strand cDNA template, primers/probes, and 2X TaqMan Fast Universal PCR Master Mix, No AmpErase UNG (Applied Biosystems). Relative quantification was performed using the comparative Ct ($2^{-}\Delta Ct$) method. ß-actin was used as internal control.

2.10. Western blot quantification of proteins extracted from tumor samples

After the end-point of *in vivo* assay, subcutaneous tumors were included in liquid nitrogen and subsequently stored at − 80 °C until their use. For protein extraction, CT+ and EE tumor samples were dissolved in RIPA (Radio-Immunoprecipitation Assay) lysis buffer (Thermo Fisher Scientific, Waltham, MA, USA) at a ratio of 100 mg sample/400 μl of RIPA. Once homogenized and sonicated, they were incubated at 4 °C for 15 min and centrifuged at 1000 g during 5 min to obtain the supernatant. Through Bradford and using albumin as a standard curve, the total proteins of the samples were quantified. For electrophoresis, 80 μg of protein from each sample (CT+ and EE) were heated at 95 °C for 5 min and separated in 10% SDS-PAGE gel in a Mini Protean II cell (Bio-Rad, Hercules, CA, USA) (100 V at 4ªC for 2 h 30 min). Proteins were transferred to a nitrocellulose membrane with a 45 μm pore size (200 V at room temperature (RT) for 1 h 15 min) (Millipore, Burlington, MA, USA) and treated with blocking solution (Phosphate- Buffered Saline (PBS)− 0.1% Tween-20 + 5% (w/v) milk powder) for 1 h. After washing three times with PBS-0.1% Tween-20, membranes were incubated with the primary antibody for 1 h (anti-caspase-8 (sc-166320), 1:1000 dilution; and anti-caspase-9 (sc-133109), 1:1000 dilution (Santa Cruz Biotechnology, Santa Cruz, CA, USA); anti-PARP1 [E102] (ab-32138), 1:2000 dilution; and anti TGF-β1 (ab-92486), 1:500 dilution (Abcam, Cambridge, UK)). After three washes, the membranes were incubated for 1 h at RT with the secondary antibody peroxidase conjugate (1:5000 dilution) (mouse anti-rabbit IgG-HRP (sc-2357) and goat anti-mouse IgG-HRP (sc-516102), Santa Cruz Biothecnology, CA, USA). Finally, anti-β-actin IgG (A3854, Sigma Aldrich, Madrid, Spain) (1:10,000 dilution) was used as an internal control. Signals were detected by an ECLTM Western blot detection reagent (Enhanced Chemiluminescence; Bonnus, Amersham, Little Chalfont, UK) [34]. Once the Western blot was performed, the bands obtained in the gels were analyzed using Quantity One analytical software (Bio-Rad, Hercules, CA, USA).

2.11. Statistical analyses

All results were carried out in triplicate and expressed as mean ± standard deviation (SD). Bivariate analyses, including Student's t-test and one-way ANOVA were applied for group comparisons. Statistical analyses were performed with Statistical Package for the Social Sciences (SPSS) v. 15.0. Differences were considered statistically significant at a p-value < 0.05.

3. Results

3.1. Euphorbia lathyris ethanolic extract blood cell toxicity

As shown in Fig. 2, EE did not induce erythrocyte agglutination even at the highest concentration tested (Fig. 2A). Moreover, the percentage of hemolysis was always less than 2%, even at a dose of 100 ug/mL, demonstrating that there was no erythrocyte toxicity (Fig. 2B). On the other hand, exposure of WBC to EE (1 and 12 h) did not induce toxicity, as the percentage of WBC proliferation for all doses tested was above 80% (Fig. 2C).

3.2. Euphorbia lathyris ethanolic extract and CRC subcutaneous tumors

3.2.1. Inhibition of subcutaneous tumor growth

C57BL/6 mice with CRC (subcutaneous induction) were used to determine the antitumor activity of EE. As shown in Fig. 3A, after 7 treatment cycles, a significant decrease in tumor size was detected in the group treated with EE relative to the control group. The decrease in tumor size was evident from the third cycle onwards.

3.2.2. Histological analysis

Subcutaneous tumors were analyzed histologically using both H&E and pentachrome methods (Fig. 3B and C). Tumors treated with EE showed less tumor cellularity and vascularization than controls (CT+). Specifically, H&E showed less nuclear staining and pentachrome images revealed an enriched collagen matrix (red), absence of red blood cells (yellow) and decrease in vasculature area in tumors treated with EE (area with blood vessels: 0,68%) relative to controls (area with blood vessels: 5.9%). In addition, cellular debris due to cell apoptosis could be observed in EE samples (necrotic area: 7.48%) in comparison with CT+ samples (no necrotic area). Moreover, tumors treated with EE were highly positive for caspase 3 staining (3.38% area), indicating an increase in apoptosis compared to controls (Fig. 3D). Finally, carbonic anhydrase analysis revealed a 35.1% activity reduction in tumors treated with EE relative to control mice (Fig. 3E). In addition, a Western blot was carried out using CT+ and EE tumor samples to quantify the expression of apoptosis-related protein (caspase 8, caspase 9, and PARP-1). As shown in Fig. 3G, a clear activation of caspase 8, 9 and PARP-1 (cleaved fractions) was detected. In addition, a significant increase in the cleaved fraction/total protein ratio in EE-treated tumors (5.16, 3.98, and 4.11-folds in caspase 8, 9, and PARP, respectively) compared to controls (CT+ tumors) was demonstrated.

3.2.3. Hematological analysis

Hematological analysis of the blood of mice before and after treatment with EE showed no significant abnormalities, indicating null toxicity of the extract (Table 1). In fact, white blood cells (WBC), hemoglobin (HGB) and platelets (PLT) reached 15,100/mm^3, 10.34 g/dL and 453,900/mm^3, respectively, in EE treated mice. These values indicate the absence of hematological toxicity in EE treated mice.

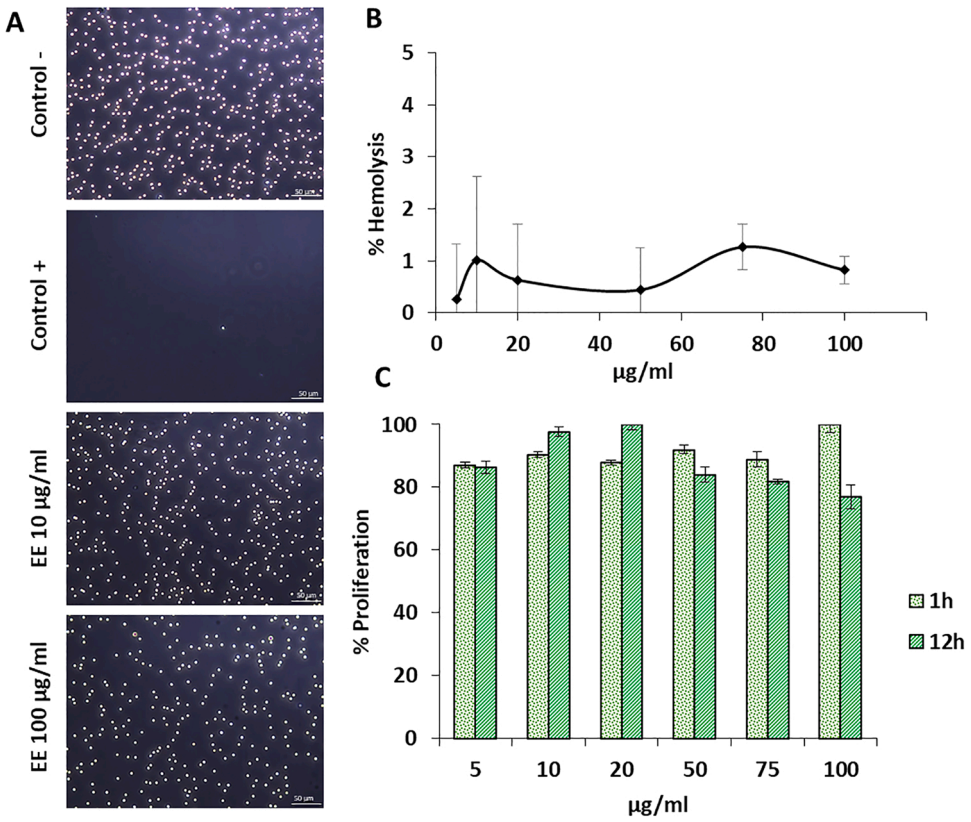

Fig. 2. Toxicity of EE in blood cells. A) Representative light microscope images of erythrocytes after treatment with EE at different concentrations (10 and 100 ug/mL). Scale bar = 25 µm. B) Percentage of erythrocyte hemolysis after treatment with EE at different concentrations. C) Toxicity of EE at different concentrations on WBCs after 1 and 12 h of treatment. Data are expressed as mean ± SD of triplicate samples.

3.3. Euphorbia lathyris ethanolic extract and CRC induced by AOM/DSS

3.3.1. Modulation of polyp size and number

C57BL/6 mice with CRC (AOM/DSS induction) were used to corroborate the antitumor activity of EE. As shown in Fig. 4, macroscopic analysis revealed a significant decrease in the number and size of polyps in the group treated with EE relative to the control group. In addition, quantification of tumor area percentage also demonstrated a significant reduction after treatment with EE. In fact, the group treated with EE showed a reduction in tumor area of more than 50% with respect to the control group.

3.3.2. Hematological analysis

Hematological analysis showed no toxicity of the extract in any of the parameters studied (Table 2). In fact, WBC, HGB and PLT reached 8250/mm^3, 15.18 g/dL and 819,220/mm^3 respectively in EE treated mice. These values indicate the absence of hematological toxicity in EE treated mice.

3.3.3. Histological analysis

As shown in Fig. 5, histological study (H&E and pentachrome staining) of Swiss roll colon samples showed significantly fewer polyps with high-grade dysplasia in the colonic mucosa of mice treated with EE than in controls (untreated CT+ mice). Dysplastic polyps are characterized by the presence of colonic epithelial cells with aberrant nuclei and abnormal colonic crypt organization without globet cells. In addition, histological studies of the spleen, lung and liver of the CT-, CT + and EE groups were performed. Pentachrome staining of spleen samples showed a large invasion of white pulp (blue) in the red pulp (olive green) in CT+, which was significantly lower in the EE group. Both H&E and pentachrome staining of lung samples showed fibrotic changes and dysplasia in the CT+ group that were not observed in the EE group. Finally, pentachrome staining of liver samples showed fibrotic changes (collagen, red) in the CT+ group that were not observed in the EE group.

3.3.4. Oxidative stress enzymes and inflammatory cytokines expression

Colon tissue samples were processed to determine the modulation of oxidative stress detoxification enzyme expression by RT-qPCR. As shown in Fig. 6, the CT + group showed a significant decrease (approx. 50%) in the expression of most of the enzymes analyzed (except GSTA) relative to the control group (CT-). Interestingly, analysis of the EE group showed a less significant decrease in enzyme expression than the CT+ group, especially in SOD2, GPX2 and NFE2L2. In addition, the levels of pro-inflammatory cytokines TNF-alpha, IL-6 and IL-1b were significantly decreased in the CT+ samples. Similar changes were found in the EE group, although it should be noted that the expression of TNF-alpha after treatment with EE was similar to that of the control.

3.3.5. Microbiome analysis

Colon tissue samples were studied to determine the modulation of the microbiome. *Lactobacillus* was the predominant genus in the CT- group. Analysis of the CT+ group demonstrated that the *Lactobacillus* genus was significantly decreased with predominant colitogenic bacteria such as *Akkermansia* (Verrucomicrobiaceae) and *Turicibacter*. However, in mice treated with EE there was a clear recovery of *Lactobacillus*, while *Turicibacter* disappeared. In addition, the presence of *Akkermansia* increased in the EE group with respect to CT+ . At the family level, *Clostridiaceae* increased in CT+ relative to CT- and significantly decreased after treatment with EE (Fig. 7).

4. Discussion

Natural products remain essential in the discovery of anticancer compounds. Some plant species are gaining great interest for CRC

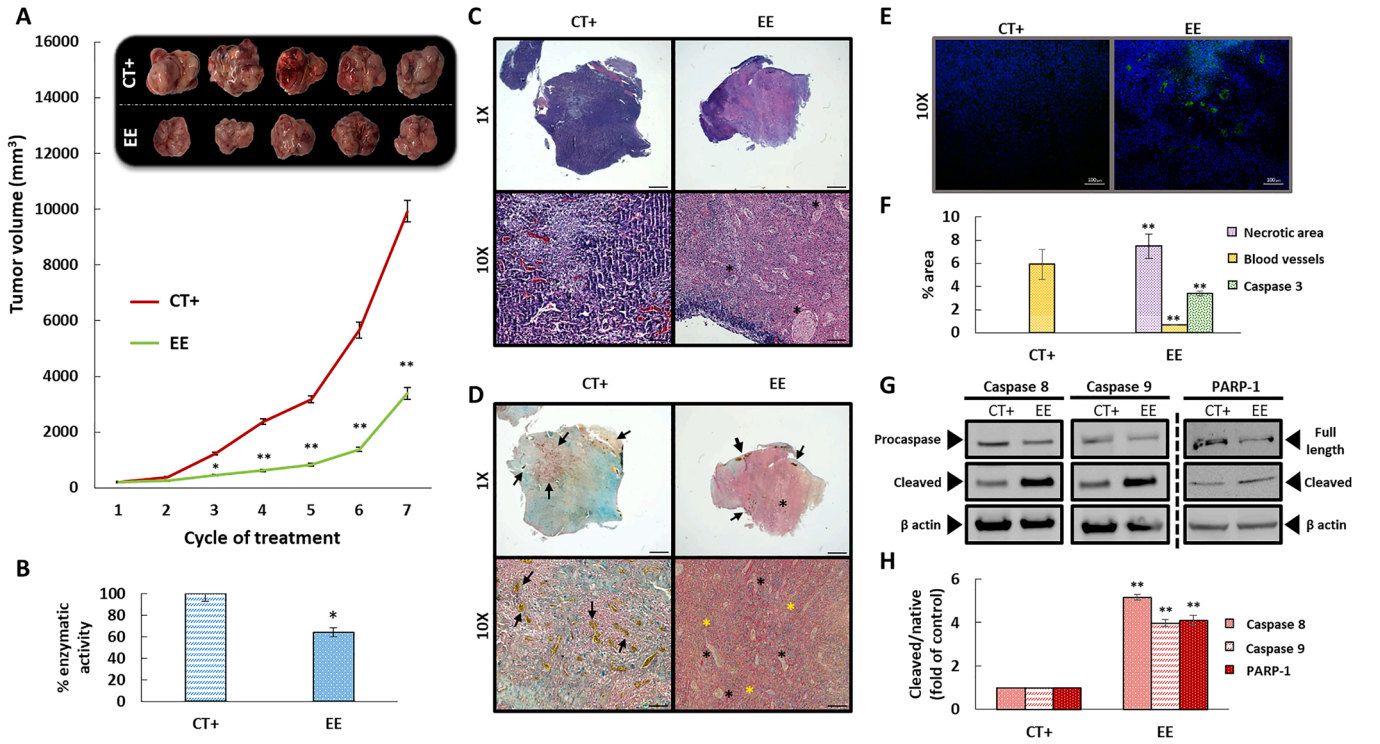

Fig. 3. *In vivo* inhibition of CRC (subcutaneous induction) growth after treatment with EE and histological analysis. A) Graphical representation of volume growth (mm^3) in colon tumors (MC38 cancer cells) in C57BL/6 mice. Mice were treated using intraperitoneal administration of EE. Untreated mice were used as control group. Data are presented as mean ± SD (n = 14). ** Significant inhibition of tumor growth comparing treatments and comparing treatments with control ($p < 0.01$). Graphical (up part) includes representative images of colon tumors obtained after euthanasia of mice at the end of the last treatment cycle. B) Graphical representation of the percentage of carbonic anhydrase enzyme activity. C) Representative images of H&E staining of tumor samples from CT + and EE groups. D) Representative images of pentachrome staining of tumor samples from CT + and EE groups. Black asterisks indicate necrotic gaps, yellow asterisks show collagen matrix, and arrows indicate blood vessels (Scale bar = 100 μm). E) Expression of apoptosis marker (caspase 3) of tumor samples from CT + and EE groups. F) Graphical representation (quantification) of necrotic area (H&E images), blood vessels (pentachrome-stained images), and caspase 3 positivity (fluorescence images). G) Western blot of caspase 8, caspase 9 and PARP-1 expression showing native and cleaved fractions. β-actin was used as an internal control. H) Quantification of caspase 8, caspase 9 and PARP-1 expression (Western blot) based on the ratio between the cleaved fraction and native protein of samples treated with EE compared to the control (CT+). Data are presented as mean ± SD; * $p < 0.05$ *vs.* control group, ** $p < 0.01$ *vs.* control group.

Table 1
Hemogram of CT+ and EE groups at the end of treatment.

Parameters	CT+(±SD)	EE (±SD)
WBC (10^3/μl)	11.15 ± 0.50	15.10 ± 0.02
RBC (10^6/μl)	4.78 ± 0.11	5.92 ± 0.13
HGB (g/dL)	8.17 ± 0.17	10.34 ± 0.18
HCT	24.81 ± 0.48	31.25 ± 0.52
PLT (10^3/μl)	700.64 ± 88.66	453.9 ± 59.42
LYM%	90.23 ± 0.36	90.75 ± 0.32
MON%	3.97 ± 0.14	3.36 ± 0.15
NEU%	4.10 ± 0.24	3.64 ± 0.17
EOS%	0.03 ± 0.00	0.02 ± 0.00
BAS%	1.67 ± 0.02	2.23 ± 0.12
MCV (fL)	52.51 ± 0.39	53.49 ± 0.46
MCH (pg)	17.24 ± 0.09	17.63 ± 0.10
RDW	17.55 ± 0.22	19.4 ± 0.34
MPV (fL)	8.24 ± 0.09	7.96 ± 0.13
PCT	0.12 ± 0.01	0.2 ± 0.02
PDW	30.91 ± 0.36	28.85 ± 1.03

WBC = Total number of white blood cells; LYM% = % of Lymphocytes; MON% = % of Monocytes/Macrophages; NEU% = % of Neutrophils/Polymorphonuclear leukocytes; EOS% = % of Eosinophils; BAS% = % of Basophils; RBC = Total number of red blood cells; HGB = Hemoglobin; HCT = % Volume of blood occupied by red blood cells (hematocrit); MCV = mean corpuscular volume; MCH = Mean corpuscular hemoglobin; PLT = Total number of platelets; MPV = Mean platelet volume; PCT = % Volume of blood occupied by platelets (thrombocrit); PDW = Platelet size distribution. Data are presented as mean ± SD.

therapy because current advances fail to achieve the expected results [35,36]. In this context, the genus Euphorbia has been studied as a source of bioactive antitumor compounds for several types of cancer [37]. However, the species *Euphorbia lathyris* and, more specifically, its seed, has not been tested. Previous *in vitro* results of our group [16] showed that the ethanolic extract from seeds of this species induced a strong *in vitro* antitumor activity against different CRC cell lines without cytotoxic effects on non-tumor cells. Therefore, this extract of *Euphorbia lathyris* was an optimal candidate for an *in vivo* study. Now, we demonstrated that EE has significant antitumor activity in the treatment of CRC both subcutaneous tumors and tumors induced in the colon mucosa with no toxicity in blood and organs.

Our results showed that EE did not cause human blood damage including WBCs or erythrocyte (no agglutination or hemolysis (<2%)), even at the highest dose tested (100 ug/mL), being far from the percentage needed (10%) to consider it a hemolytic compound [38,39]. This relevant result differentiated the *Euphorbia lathyris* extract from other Euphorbia genera that have shown severe toxicity. In fact, Adedapo et al. [40] showed the deleterious effect of *Euphorbia hirtha* on rat serum biochemistry, and Al-Sultan and Yehia [41] documented the harmful effect of *Euphorbia heliscopia* on different rat organs. Furthermore, prolonged exposures of rats to a methanolic extract of *Euphorbia peplus* negatively affected heart and kidney tissue, probably due to its inflammatory and apoptotic activity [42]. Conversely, EE did not induce blood or organ lesions in mice after *in vivo* assays, supporting its lack of toxicity. In fact, hemogram parameters remain unchanged before and after EE treatment, corroborating the previous study that was performed

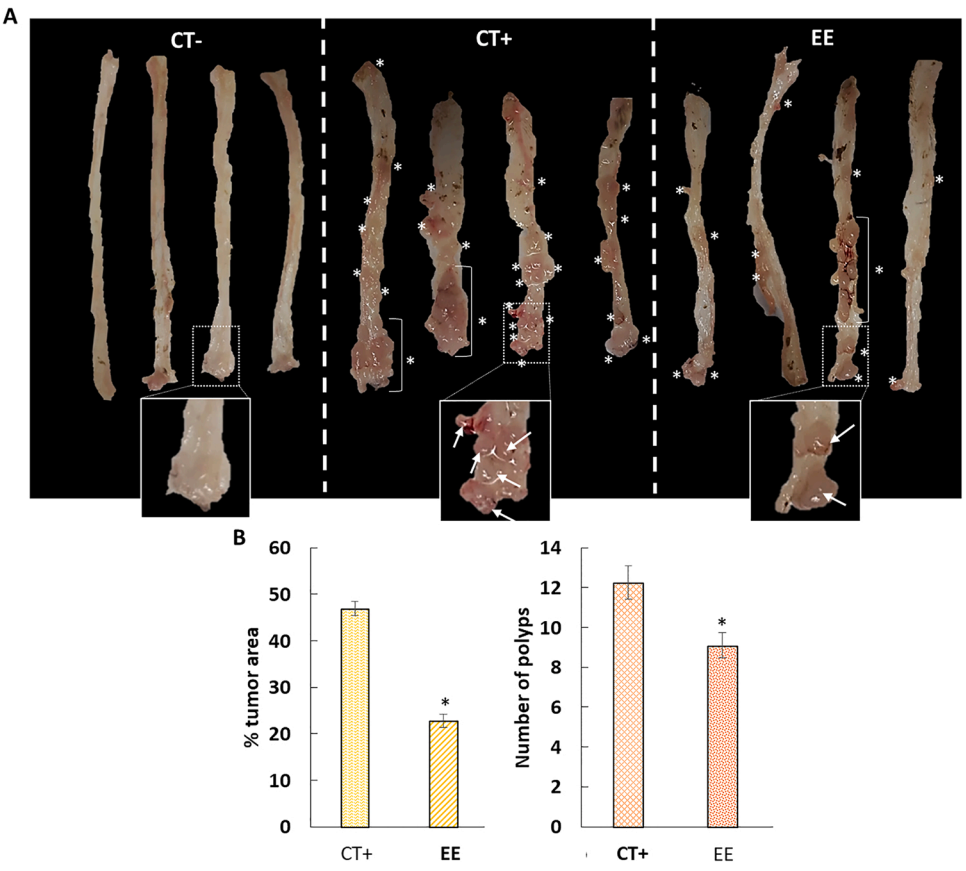

Fig. 4. *In vivo* inhibition of CRC (AOM/DSS induction) growth after treatment with EE. A) Representative image of the dissected colon of four mice after completion of the *in vivo* experiment. White asterisks mark polyp formation along the intestine. B) Graphical representation of the percentage of tumor area and number of polyps in the groups treated with *Euphorbia lathyris* (EE) and the control group (CT+). Data are presented as mean ± SD (n = 14 for CT+ and EE groups, n = 5 for CT- group). * $p < 0.05$ *vs.* control group.

Table 2
Hemogram from CT-, CT+ and EE groups before the end of the experiment.

Parameters	CT- (x ± SD)	CT+ (x ± SD)	EE (x ± SD)
WBC (10^3/μl)	9.86 ± 1.00	6.97 ± 0.94	8.25 ± 1.23
RBC (10^6/μl)	10.22 ± 0.88	7.89 ± 1.31	9.77 ± 0.26
HGB (g/dL)	16.08 ± 1.31	12.6 ± 1.13	15.18 ± 0.53
HCT	46.43 ± 3.79	38.32 ± 2.80	44.27 ± 1.75
PLT (10^3/μl)	672.44 ± 97.01	430.92 ± 54.33	819.22 ± 108.1
LYM%	95.13 ± 0.95	93.04 ± 1.28	94.37 ± 0.72
MON%	0.39 ± 0.06	0.94 ± 0.07	0.4 ± 0.09
NEU%	3.81 ± 1.02	4.83 ± 0.09	4.5 ± 0.84
EOS%	0.24 ± 0.05	0.1 ± 0.00	0.07 ± 0.03
BAS%	0.44 ± 0.16	1.08 ± 0.26	0.66 ± 0.14
MCV (fL)	45.49 ± 1.46	48.93 ± 4.63	45.32 ± 0.62
MCH (pg)	15.77 ± 0.46	16.11 ± 1.21	15.53 ± 0.15
RDW	14.01 ± 0.50	16.41 ± 2.34	14.39 ± 0.81
MPV (fL)	5.88 ± 0.07	7.88 ± 0.81	5.88 ± 0.04
PCT	0.43 ± 0.11	0.19 ± 0.13	0.48 ± 0.06
PDW	22.3 ± 3.26	35.3 ± 8.91	21.04 ± 1.55

WBC = Total number of white blood cells; LYM% = % of Lymphocytes; MON% = % of Monocytes/Macrophages; NEU% = % of Neutrophils/Polymorphonuclear leukocytes; EOS% = % of Eosinophils; BAS% = % of Basophils; RBC = Total number of red blood cells; HGB = Hemoglobin; HCT = % Volume of blood occupied by red blood cells (hematocrit); MCV = mean corpuscular volume; MCH = Mean corpuscular hemoglobin; PLT = Total number of platelets; MPV = Mean platelet volume; PCT = % Volume of blood occupied by platelets (thrombocrit); PDW = Platelet size distribution. Data are presented as mean ± SD.

in human blood cells. Moreover, histological studies using pentachrome and H&E staining after EE treatment showed absence of lesions (lung and liver samples) or low severe lesions (spleen samples).

In vivo assays using two murine CRC models clearly demonstrated that EE treatment was effective in this type of tumor. First, volume of heterotopic xenograft tumors (subcutaneous tumors) significantly decreased after treatment with EE. In fact, a significant volume reduction was observed from the third dose applied. Histological analysis of tumor samples after EE treatment showed a marked decrease in the cellular component of tumors, which was replaced by a fibrous matrix. In fact, pentachrome images clearly showed high red staining, indicating the presence of collagen leading to intense fibrosis. Moreover, histochemical analysis (pentachrome staining) demonstrated an antiangiogenic effect of EE supported by the absence of blood vessels in treated tumor samples relative to untreated samples. Interestingly, this antiangiogenic activity was supported by previous *in vitro* results using HUVEC cells [16], and could be related to the demonstrated presence of esculetin in EE [16], a molecule capable of inhibiting VEGF-induced angiogenesis both *in vitro* and *in vivo* (Park et al. [43]). Regarding the antitumor mechanism induced by EE *in vivo*, our results supported that apoptosis was mediated by caspase 3, 8 and 9, as shown by immunofluorescence and Western blot analyses in tumor samples after treatment with EE. However, a clear inhibition of carbonic anhydrase activity was also observed. This enzymatic activity could be related to the presence of esculetin in EE, which has been demonstrated to inhibit tumor carbonic anhydrase [44,45]. This mechanism could be one of the triggers of tumor apoptosis activated by EE in our samples. Second, the use of a mouse model with AOM/DSS-induced tumors confirmed the antitumor activity of treatment with EE. Swiss roll histological images revealed successful induction of dysplastic polyps (cancer precursor lesions) in the colonic mucosa of mice. Interestingly, EE treatment significantly decreased these lesions with respect to untreated mice. These results suggest that EE treatment might not only have antitumor activity against colon tumors but also a preventive effect on the development of cancer precursor lesions (*i.e.*, dysplastic polyps). In fact, this effect could also be related to the presence of esculetin in the extract, since this molecule

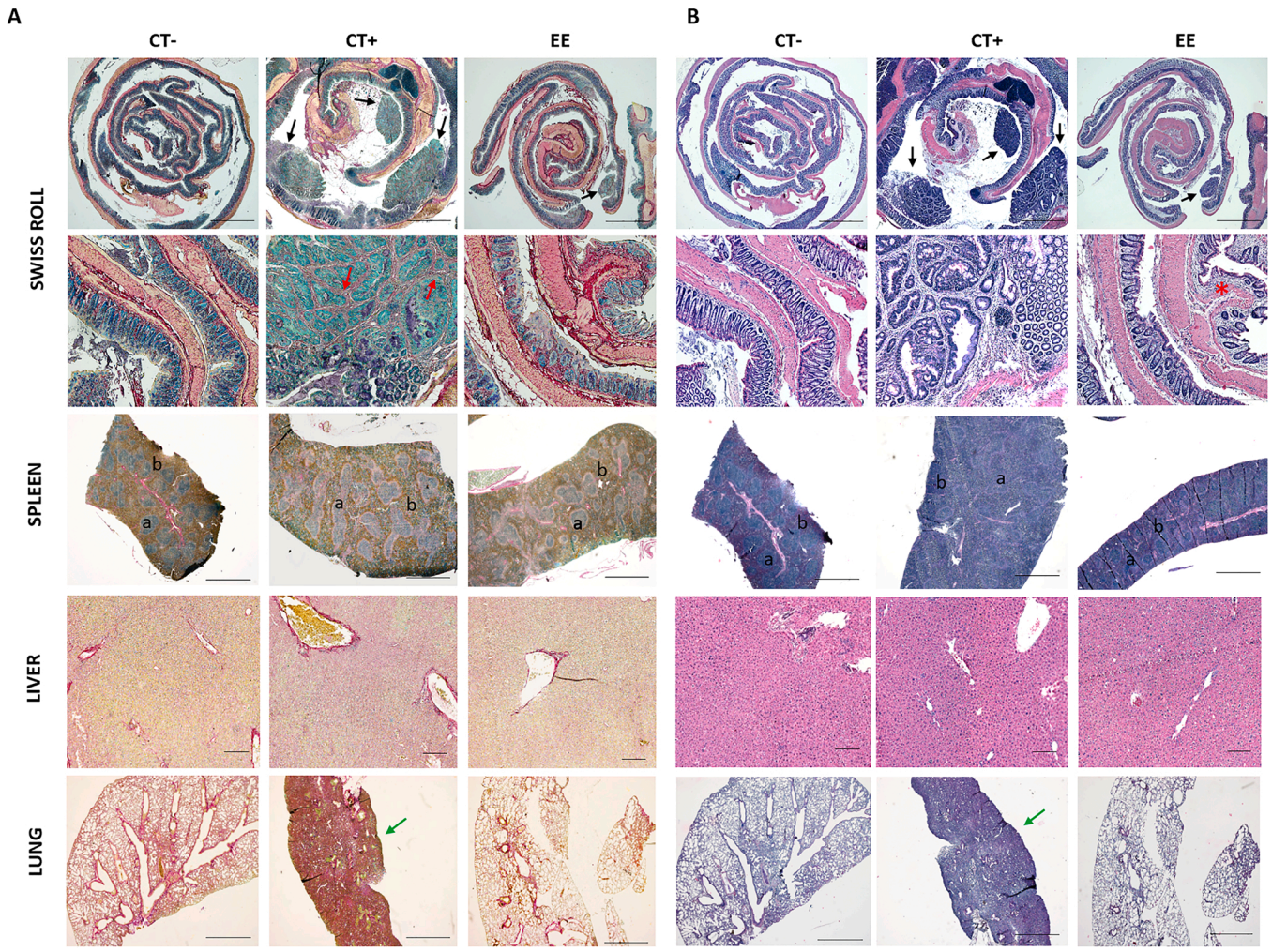

Fig. 5. Representative images of histological stains after tumor induction by AOM/DSS. The Swiss roll technique was used to analyze colon of treated (EE), untreated (CT+) and control (CT-) groups. Pentachrome (A) and H&E staining (B) of colon (Swiss roll) (scale bar = 1000 μm (upper) and 100 μm (lower)) spleen (scale bar = 1000 μm), liver (scale bar = 100 μm) and lung samples (scale bar = 1000 μm). Pentachrome staining shows dysplastic polyps as a green structure without globet cells (violet) (black arrows) and with some collagen fibrous tracts (red arrows). H&E staining showing the presence of polyps with dysplasia (red asterisks). Spleen samples show white pulp (a) and red pulp (b). In the case of CT + samples, invasion of white pulp into red pulp was observed, being less marked in the case of EE samples. Liver samples showed fibrotic changes (collagen) (red) in the CT + group that were not observed in the EE and CT- groups. Lung samples from the CT+ group showed fibrotic areas (green arrows) that did not appear in the EE and CT- groups.

was able to inhibit the formation of the β-catenin/Tcf complex, a crucial pathway to the formation of dysplastic polyps, both *in vitro* and *in vivo* studies [46].

On the other hand, EE treatment induced relevant changes in microbiota, oxidative stress enzymes and pro-inflammatory cytokines in the colon tissue of AOM/DSS-induced tumors. Our results showed a significant increase in colitogenic and dysbiotic bacteria (*Akkermansia*, *Turicibacter* and *Clostridiaceae*) [47,48], and a decrease in eubiotic bacteria (*Lactobacillus*) in the colon of mice with AOM/DSS-induced tumors (CT+ group) compared to the control group (CT-). These changes may be explained by inflammatory processes involving the colonic mucosa. On the contrary, the colon of mice treated with EE showed increased numbers of *Lactobacillus* and absence of *Turicibacter* and *Clostridiaceae* relative to the CT+ group. Recently, the regulation of gut microbiota (including an increase in *Lactobacillus* in the colon) induced by evodiamine, an extract from the plant genus *Tetradium*, was associated with inhibition of CRC development [49]. In addition, the increase in *Lactobacillus* by the use of a prebiotic has been related to a reduction in the risk of colitis-associated colon cancer [27]. On the other hand, *Akkermansia* paradoxically increased in groups treated with EE with respect to the CT+ group. This could be explained on the grounds that the presence of *Akkermansia* in human colonic microbiota has been related to increased responses to anti-PD-1/PDL-1 immunotherapy due to the similarity between *Akkermansia* and some tumor antigens [50].

Finally, RT-qPCR analyses revealed low expression of oxidative stress enzymes and pro-inflammatory cytokines in the colon of specimens from the CT + group, which contrasted with the elevated levels of the same enzymes after treatment with EE. Exposure of the colonic mucosa to AOM/DSS induces oxidative stress and epithelial damage [51] leading to depletion of antioxidant enzymes such as GPX, SOD or CAT [52]. As shown in Fig. 8, we hypothesized that depletion of these enzymes could induce an arrest of the inflammatory response. This fact was supported by the decreased expression of cytokines (TNF-alpha, IL-6 and IL-1b), suggesting the development of a protective mechanism against oxidative and inflammatory immunological stress in the colonic mucosa with lack of detoxification enzymes. Interestingly, after treatment with EE, higher levels of oxidative stress enzymes in the colon mucosa were detected, probably associated with increased innate and inflammatory response [53]. In fact, we observed high levels of TNF-alpha and some oxidative stress enzymes in mice treated with EE. Considering that innate immunity and inflammatory cytokines are the first step for tumor antigen presentation and cytotoxic T cell response

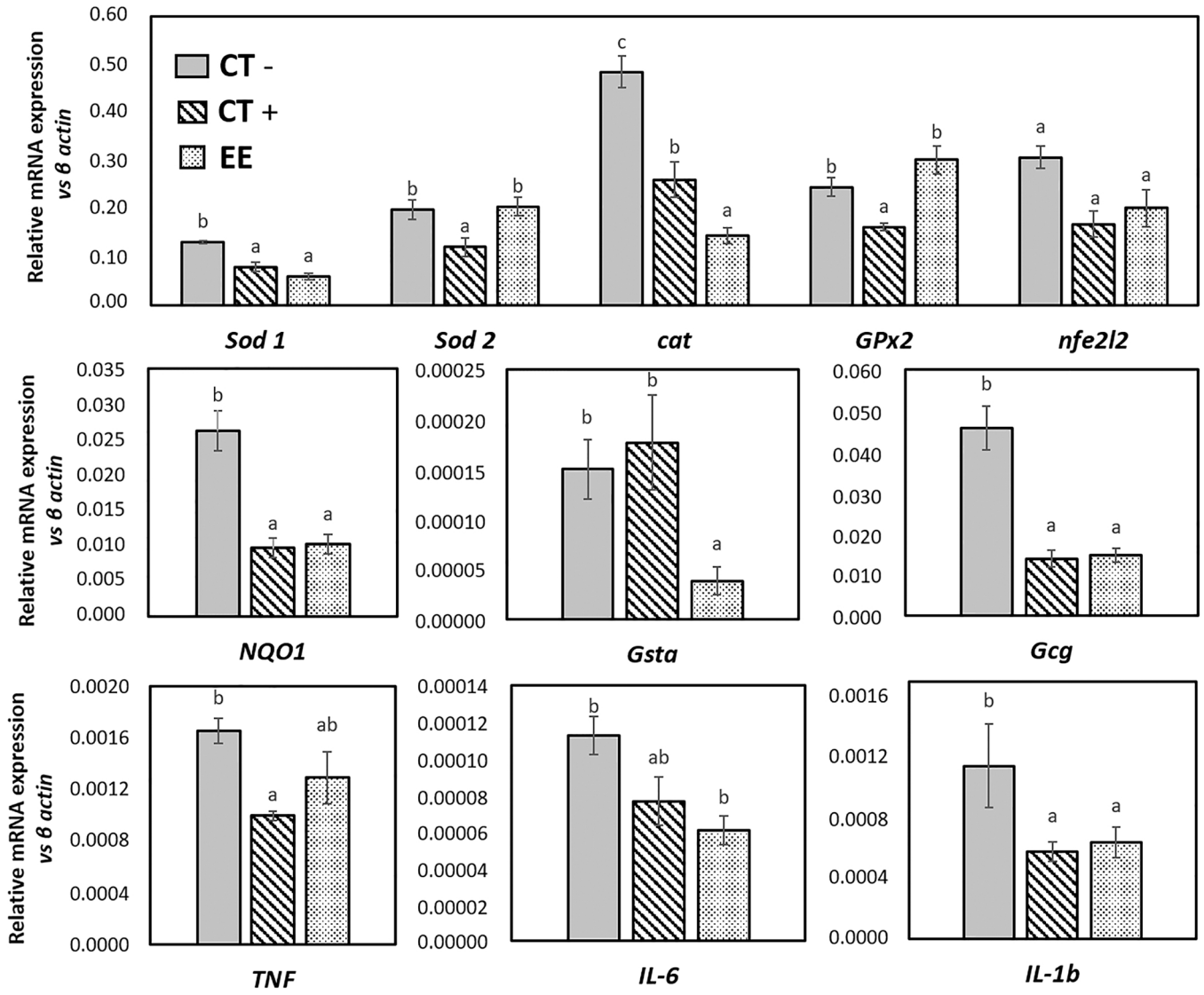

Fig. 6. Expression of oxidative stress enzymes and inflammatory cytokines in colon samples. Graphical representation of relative mRNA expression of enzymes SOD1, SOD2, CAT, GPX2, NFE2L2, NQO1, GSTA and GCG, and cytokines TNF-alpha, IL-6 and IL-1b in colon samples from CT-, CT+ and EE groups. Bars with different letters (a,b,c) denote significant differences ($p < 0.05$) among experimental groups.

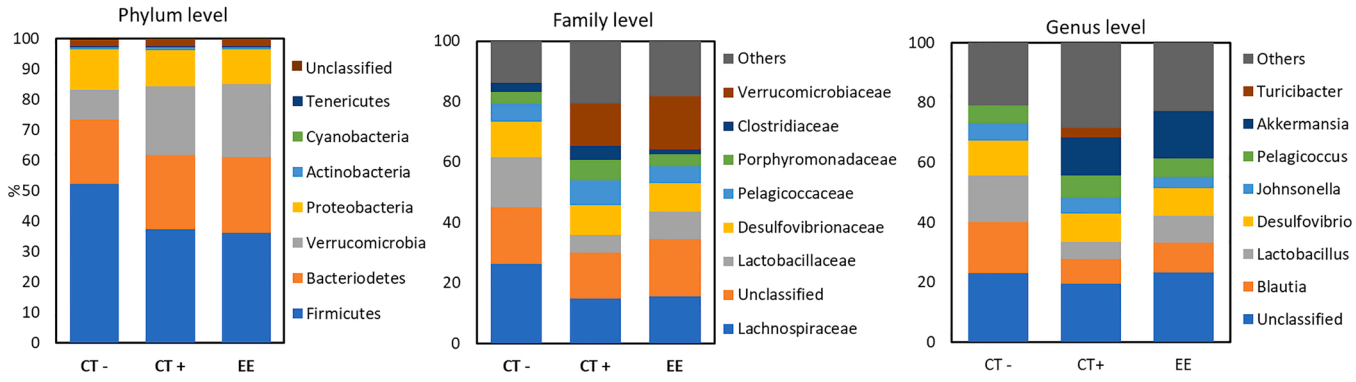

Fig. 7. Colon microbiome analysis. Percentage of different bacteria at the phylum, family and genus levels in colon samples from CT-, CT+ and EE groups. Data represent the mean values of triplicate samples.

[54], inactivation of innate immunity by AOM/DSS could be involved in the development of dysplastic polyps due to lack of tumor antigen presentation [55]. In this context, treatment with EE could allow an increased level of antigen presentation and, thus, an enhanced T cell cytotoxic response that could help to destroy and reduce new dysplastic polyps, as we demonstrated in *in vivo* assays.

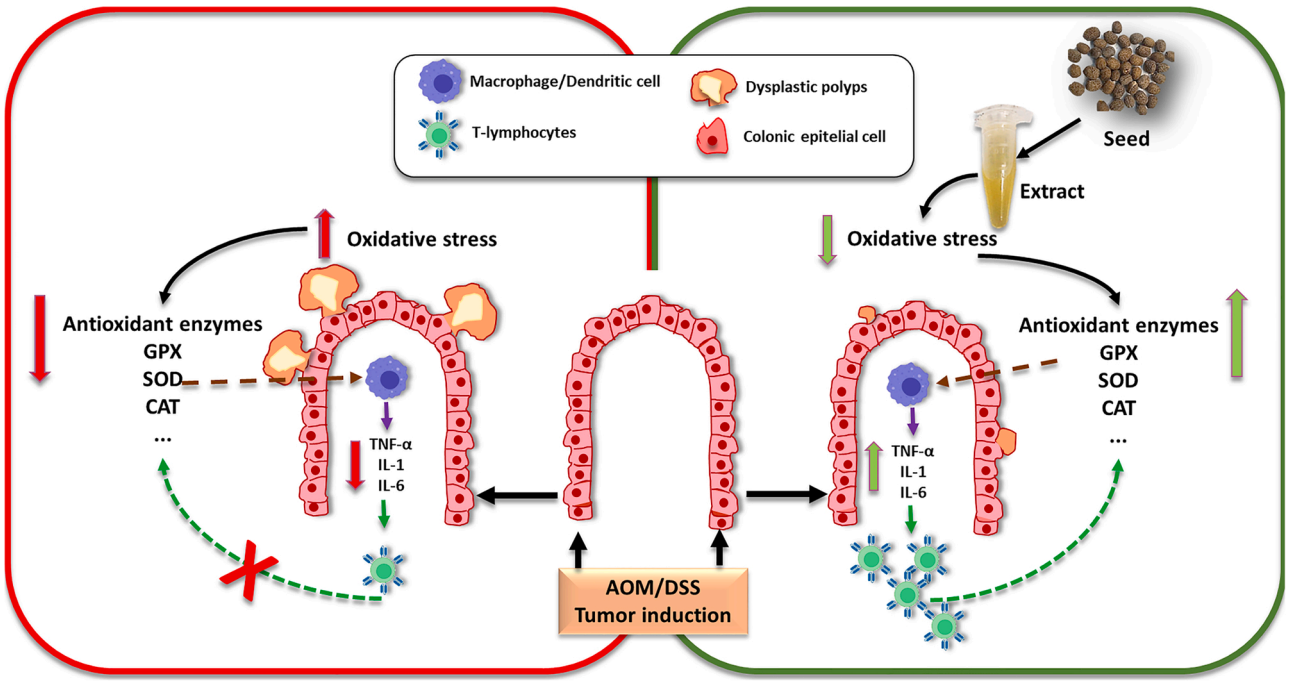

Fig. 8. Schematic illustration summarizing a possible relationship between the innate/inflammatory immune system and colonic epithelia due to increased oxidative stress levels and expression of antioxidant enzymes. Left: AOM/DSS induces oxidative stress along with depletion of antioxidant enzymes. Decreased expression of cytokines reduces the immune response against the colonic mucosa. Right: EE treatment increases the expression of oxidative stress enzymes in the colonic mucosa. The presence of elevated levels of cytokines increases the immune response, inducing a decrease in dysplastic polyps.

The relationship between oxidative stress, inflammatory stress and intestinal microbiota has been recently described by Alemany-Cosme et al. [56] who indicate that dysbiotic gut microbiota increases oxidative stress and inflammatory cytokines and predispose to inflammatory bowel diseases such as Crohn's disease. In our study, EE-treated mice showed a decrease in colitogenic bacteria such as Turicibacter and Clostridiaceae, and recovery of eubiotic bacteria such as Lactobacillus. Therefore, EE could also modulate and decrease the oxidative and inflammatory intestinal stress induced by a dysbiotic microbiome [56].

5. Conclusions

Our results showed for the first time that an ethanolic extract from mature seeds of Euphorbia lathyris (variety S3201), which previously showed *in vitro* antiproliferative activity against colon cancer cells, induced a potent *in vivo* antitumor effect in CRC that was corroborated in both heterotopic xenograft and AOM/DSS-induced colon models. Treatment with EE was able to significantly reduce the volume of subcutaneous tumors. In addition, this treatment decreased dysplastic polyps in the colonic mucosa, suggesting a preventive effect and increased antioxidant enzymes and promoted a eubiotic environment in the colonic mucosa. These results suggest that EE may be a new strategy to improve CRC treatment and would be a strong candidate for future human clinical trials.

Funding

This research was funded by the Spanish Ministry of Science, Innovation, and Universities through projects RTC-2017-6540-1, RTC2019-006870-1, Junta de Andalucía through project P18-TP-1420 and FEDER Program. In addition, this work was supported by funds from research groups AGR145 and CTS-107 (Andalusian Government).

CRediT authorship contribution statement

C. Mesas: Conceptualization, Formal analysis, Supervision, Writing – review & editing, Funding acquisition. **R. Martínez:** Investigation, Formal analysis, Writing – original draft. **K. Doello:** Investigation, Writing – original draft. **R. Ortiz:** Investigation. **M. López-Jurado:** Formal analysis. **Francisco Bermúdez:** Conceptualization, Resources, Funding acquisition. **F. Quiñonero:** Investigation. **J. Prados:** Conceptualization, Writing – review & editing, Funding acquisition. **J.M. Porres:** Conceptualization, Supervision, Writing – review & editing, Funding acquisition. **C. Melguizo:** Investigation, Writing – original draft. All authors have read and approved the final manuscript.

Conflict of interest statement

The authors declare no conflict of interest.

Acknowledgments

The authors want to thank Antonio Murillo Cancho from the University of Almería and CELLBITEC S.L.

References

[1] A. Recio-Boiles, B. Cagir, Colon Cancer, in: StatPearls, StatPearls Publishing, Treasure Island (FL), 2021. ⟨http://www.ncbi.nlm.nih.gov/books/NBK470380/⟩ (Accessed 9 October 2021).
[2] H. Sung, J. Ferlay, R.L. Siegel, M. Laversanne, I. Soerjomataram, A. Jemal, F. Bray, Global Cancer Statistics 2020: GLOBOCAN Estimates of Incidence and Mortality Worldwide for 36 Cancers in 185 Countries, CA Cancer J. Clin. 71 (2021) 209–249, https://doi.org/10.3322/caac.21660.
[3] C. Tiselius, A. Rosenblad, E. Strand, K. Smedh, Risk factors for poor health-related quality of life in patients with colon cancer include stoma and smoking habits, Health Qual. Life Outcomes 19 (2021) 216, https://doi.org/10.1186/s12955-021-01850-5.
[4] P. Moleyar-Narayana, S. Ranganathan, Cancer Screening, in: StatPearls, StatPearls Publishing, Treasure Island (FL), 2021. ⟨http://www.ncbi.nlm.nih.gov/books/NBK563138/⟩ (Accessed 12 November 2021).
[5] E.J. Kuipers, W.M. Grady, D. Lieberman, T. Seufferlein, J.J. Sung, P.G. Boelens, C.J. H. van de Velde, T. Watanabe, Colorectal cancer, Nat. Rev. Dis. Prim. 1 (2015) 15065, https://doi.org/10.1038/nrdp.2015.65.
[6] R.V. Groehs, M.V. Negrao, L.A. Hajjar, C.P. Jordão, B.P. Carvalho, E. Toschi-Dias, A.C. Andrade, F.P. Hodas, M.J.N.N. Alves, A.O. Sarmento, L. Testa, P.M.G. Hoff, C.

E. Negrao, R.K. Filho, Adjuvant treatment with 5–fluorouracil and oxaliplatin does not influence cardiac function, neurovascular control, and physical capacity in patients with colon cancer, Oncologist 25 (2020), e13475, https://doi.org/10.1634/theoncologist.2020-0225.
[7] A. Fernández Montes, N. Martínez Lago, M. Covela Rúa, J. de la Cámara Gómez, P. González Villaroel, J.C. Méndez Méndez, M. Jorge Fernández, M. Salgado Fernández, M. Reboredo López, G. Quintero Aldana, M. Luz Pellón Augusto, B. Graña Suárez, J. García Gómez, Efficacy and safety of FOLFIRI/aflibercept in second-line treatment of metastatic colorectal cancer in a real-world population: prognostic and predictive markers, Cancer Med. 8 (2019) 882–889, https://doi.org/10.1002/cam4.1903.
[8] R. Gupta, L.K. Bhatt, T.P. Johnston, K.S. Prabhavalkar, Colon cancer stem cells: potential target for the treatment of colorectal cancer, Cancer Biol. Ther. 20 (2019) 1068–1082, https://doi.org/10.1080/15384047.2019.1599660.
[9] M.G. Guren, The global challenge of colorectal cancer, Lancet Gastroenterol. Hepatol. 4 (2019) 894–895, https://doi.org/10.1016/S2468-1253(19)30329-2.
[10] F. Morano, F. Sclafani, Duration of first-line treatment for metastatic colorectal cancer: Translating the available evidence into general recommendations for routine practice, Crit. Rev. Oncol. Hematol. 131 (2018) 53–65, https://doi.org/10.1016/j.critrevonc.2018.08.006.
[11] E. Dekker, P.J. Tanis, J.L.A. Vleugels, P.M. Kasi, M.B. Wallace, Colorectal cancer, Lancet 394 (2019) 1467–1480, https://doi.org/10.1016/S0140-6736(19)32319-0.
[12] A. Dehal, A.N. Graff-Baker, B. Vuong, T. Fischer, S.J. Klempner, S.-C. Chang, G. L. Grunkemeier, A.J. Bilchik, M. Goldfarb, Neoadjuvant chemotherapy improves survival in patients with clinical T4b colon cancer, J. Gastrointest. Surg. 22 (2018) 242–249, https://doi.org/10.1007/s11605-017-3566-z.
[13] W.R. Bidlack, S.T. Omaye, M.S. Meskin, D.K.W. Topham, eds., Phytochemicals as Bioactive Agents, CRC Press, Boca Raton, 2014. ⟨https://doi.org/10.1201/9781482278880⟩.
[14] S. Goyal, N. Gupta, S. Chatterjee, S. Nimesh, Natural plant extracts as potential therapeutic agents for the treatment of cancer, Curr. Top. Med. Chem. 17 (2017) 96–106, https://doi.org/10.2174/1568026616666160530154407.
[15] M. Ernst, C.H. Saslis-Lagoudakis, O.M. Grace, N. Nilsson, H.T. Simonsen, J. W. Horn, N. Rønsted, Evolutionary prediction of medicinal properties in the genus Euphorbia L, Sci. Rep. 6 (2016) 30531, https://doi.org/10.1038/srep30531.
[16] C. Mesas, R. Martínez, R. Ortíz, M. Galisteo, M. López-Jurado, L. Cabeza, G. Perazzoli, C. Melguizo, J.M. Porres, J. Prados, Antitumor effect of the ethanolic extract from seeds of euphorbia lathyris in colorectal cancer, Nutrients 13 (2021) 566, https://doi.org/10.3390/nu13020566.
[17] J. Wei, L. Lu, D. Mei-cai, S. Hua-wu, L. Run-hua, Studies on chemical constituents in seeds of Euphorbia lathyris., Undefined, 2010. /paper/Studies-on-chemical-constituents-in-seeds-of-Wei-Lu/0f0d005bf5458cfd897c2535a24db7c7cd5a934f (Accessed 3 December 2020).
[18] Y.N. Teng, Y. Wang, P.L. Hsu, G. Xin, Y. Zhang, S.L. Morris-Natschke, M. Goto, K. H. Lee, Mechanism of action of cytotoxic compounds from the seeds of Euphorbia lathyris, Phytomedicine 41 (2018) 62–66, https://doi.org/10.1016/j.phymed.2018.02.001.
[19] C. Bicchi, G. Appendino, C. Cordero, P. Rubiolo, D. Ortelli, J.L. Veuthey, HPLC-UV and HPLC-positive-ESI-MS analysis of the diterpenoid fraction from caper spurge (Euphorbia lathyris) seed oil, Phytochem. Anal. 12 (2001) 255–262, https://doi.org/10.1002/pca.592.
[20] G. Appendino, C. Della Porta, G. Conseil, O. Sterner, E. Mercalli, C. Dumontet, A. Di Pietro, A new P-glycoprotein inhibitor from the caper spurge (Euphorbia lathyris), J. Nat. Prod. 66 (2003) 140–142, https://doi.org/10.1021/np0203537.
[21] M. Ernst, O.M. Grace, C.H. Saslis-Lagoudakis, N. Nilsson, H.T. Simonsen, N. Rønsted, Global medicinal uses of Euphorbia L. (Euphorbiaceae), J. Ethnopharmacol. 176 (2015) 90–101, https://doi.org/10.1016/j.jep.2015.10.025.
[22] L. Fan, H. Zhu, W. Tao, L. Liu, X. Shan, M. Zhao, D. Sun, Euphorbia factor L2 inhibits TGF-β-induced cell growth and migration of hepatocellular carcinoma through AKT/STAT3, Phytomedicine 62 (2019), 152931, https://doi.org/10.1016/j.phymed.2019.152931.
[23] Y. Wang, X. Yu, L. Wang, F. Zhang, Y. Zhang, Research progress on chemical constituents and anticancer pharmacological activities of euphorbia lunulata bunge, BioMed. Res. Int. 2020 (2020), e3618941, https://doi.org/10.1155/2020/3618941.
[24] G. Williamson, M.N. Clifford, Role of the small intestine, colon and microbiota in determining the metabolic fate of polyphenols, Biochem. Pharmacol. 139 (2017) 24–39, https://doi.org/10.1016/j.bcp.2017.03.012.
[25] K. Pandey, S. Umar, Microbiome in drug resistance to colon cancer, Curr. Opin. Physiol. 23 (2021), 100472, https://doi.org/10.1016/j.cophys.2021.100472.
[26] W.H. Lee, K.P. Chen, K. Wang, H.C. Huang, H.F. Juan, Characterizing the cancer-associated microbiome with small RNA sequencing data, Biochem. Biophys. Res. Commun. 522 (2020) 776–782, https://doi.org/10.1016/j.bbrc.2019.11.166.
[27] N.S. Oh, J.Y. Lee, Y.T. Kim, S.H. Kim, J.H. Lee, Cancer-protective effect of a synbiotic combination between Lactobacillus gasseri 505 and a Cudrania tricuspidata leaf extract on colitis-associated colorectal cancer, Gut Microbes 12 (2020), 1785803, https://doi.org/10.1080/19490976.2020.1785803.
[28] Y. Zhao, Q. Jiang, Roles of the polyphenol-gut microbiota interaction in alleviating colitis and preventing colitis-associated colorectal cancer, Adv. Nutr. 12 (2021) 546–565, https://doi.org/10.1093/advances/nmaa104.
[29] J. Jiménez-López, M.M. El-Hammadi, R. Ortiz, M.D. Cayero-Otero, L. Cabeza, G. Perazzoli, L. Martin-Banderas, J.M. Baeyens, J. Prados, C. Melguizo, A novel nanoformulation of PLGA with high non-ionic surfactant content improves in vitro and in vivo PTX activity against lung cancer, Pharmacol. Res. 141 (2019) 451–465, https://doi.org/10.1016/j.phrs.2019.01.013.
[30] Y. Jabalera, B. Garcia-Pinel, R. Ortiz, G. Iglesias, L. Cabeza, J. Prados, C. Jimenez-Lopez, C. Melguizo, Oxaliplatin-biomimetic magnetic nanoparticle assemblies for colon cancer-targeted chemotherapy: an in vitro study, Pharmaceutics 11 (2019), E395, https://doi.org/10.3390/pharmaceutics11080395.
[31] A.B. Bialkowska, A.M. Ghaleb, M.O. Nandan, V.W. Yang, Improved swiss-rolling technique for intestinal tissue preparation for immunohistochemical and immunofluorescent analyses, J. Vis. Exp. (2016), https://doi.org/10.3791/54161.
[32] K. Doello, A. New, Pentachrome method for the simultaneous staining of collagen and sulfated mucopolysaccharides, Yale J. Biol. Med. 87 (2014) 341–347.
[33] C.S. Gai, J. Lu, C.J. Brigham, A.C. Bernardi, A.J. Sinskey, Insights into bacterial CO_2 metabolism revealed by the characterization of four carbonic anhydrases in Ralstonia eutropha H16, AMB Express 4 (2014) 2, https://doi.org/10.1186/2191-0855-4-2.
[34] R. Ortiz, J. Prados, C. Melguizo, A.R. Rama, A. Segura, F. Rodríguez-Serrano, H. Boulaiz, F. Hita, A. Martinez-Amat, R. Madeddu, J.L. Ramos, A. Aranega, The cytotoxic activity of the phage E protein suppress the growth of murine B16 melanomas in vitro and in vivo, J. Mol. Med. 87 (2009) 899–911, https://doi.org/10.1007/s00109-009-0493-9.
[35] T. Sen, S.K. Samanta, Medicinal plants, human health and biodiversity: a broad review, Adv. Biochem. Eng. Biotechnol. 147 (2015) 59–110, https://doi.org/10.1007/10_2014_273.
[36] A. Niedzwiecki, M.W. Roomi, T. Kalinovsky, M. Rath, Anticancer efficacy of polyphenols and their combinations, Nutrients 8 (2016), E552, https://doi.org/10.3390/nu8090552.
[37] F. Cateni, G. Falsone, J. Zilic, Terpenoids and glycolipids from euphorbiaceae, Mini Rev. Med. Chem. 3 (2003) 425–437, https://doi.org/10.2174/1389557033487971.
[38] K. Amin, R.-M. Dannenfelser, In vitro hemolysis: guidance for the pharmaceutical scientist, J. Pharm. Sci. 95 (2006) 1173–1176, https://doi.org/10.1002/jps.20627.
[39] M. Podsiedlik, M. Markowicz-Piasecka, J. Sikora, Erythrocytes as model cells for biocompatibility assessment, cytotoxicity screening of xenobiotics and drug delivery, Chem. Biol. Interact. 332 (2020), 109305, https://doi.org/10.1016/j.cbi.2020.109305.
[40] A.A. Adedapo, M.O. Abatan, O.O. Olorunsogo, Toxic effects of some plants in the genus Euphorbia on haematological and biochemical parameters of rats, Vet. Arh. 74 (2004) 53–62.
[41] S.I. Al-sultan, Y.A. Hussein, Acute Toxicity of Euphorbia heliscopia in Rats, (n.d.).
[42] Y.M. Abd-Elhakim, M. Abdo Nassan, G.A. Salem, A. Sasi, A. Aldhahrani, K. Ben Issa, A. Abdel-Rahman Mohamed, Investigation of the in-vivo cytotoxicity and the in silico-prediction of MDM2-p53 inhibitor potential of euphorbia peplus methanolic extract in rats, Toxins 11 (2019), E642, https://doi.org/10.3390/toxins11110642.
[43] S.L. Park, S.Y. Won, J.-H. Song, S.-Y. Lee, W.-J. Kim, S.-K. Moon, Esculetin inhibits VEGF-induced angiogenesis both in vitro and in vivo, Am. J. Chin. Med. 44 (2016) 61–76, https://doi.org/10.1142/S0192415×1650004X.
[44] W. Na, Y.H. Kang, Aesculetin inhibits bone resorption through down-regulating differentiation and lysosomal formation in osteoclasts, Curr. Dev. Nutr. 4 (2020) 442, https://doi.org/10.1093/cdn/nzaa045_075.
[45] I. Basaran, S. Sinan, U. Cakir, M. Bulut, O. Arslan, O. Ozensoy, In vitro inhibition of cytosolic carbonic anhydrases I and II by some new dihydroxycoumarin compounds, J. Enzym. Inhib. Med. Chem. 23 (2008) 32–36, https://doi.org/10.1080/14756360701404100.
[46] S.Y. Lee, T.G. Lim, H. Chen, S.K. Jung, H.J. Lee, M.H. Lee, D.J. Kim, A. Shin, K. W. Lee, A.M. Bode, Y.-J. Surh, Z. Dong, Aesculetin suppresses proliferation of human colon cancer cells by directly targeting β-catenin, Cancer Prev. Res. (Philos.) 6 (2013), https://doi.org/10.1158/1940-6207.CAPR-13-0241.
[47] C. Howe, S.J. Kim, J. Mitchell, E. Im, Y.S. Kim, Y.S. Kim, S.H. Rhee, Differential expression of tumor-associated genes and altered gut microbiome with decreased Akkermansia muciniphila confer a tumor-preventive microenvironment in intestinal epithelial Pten-deficient mice, Biochim. Biophys. Acta (BBA) - Mol. Basis Dis. 1864 (2018) 3746–3758, https://doi.org/10.1016/j.bbadis.2018.10.006.
[48] M. Wu, J. Li, Y. An, P. Li, W. Xiong, J. Li, D. Yan, M. Wang, G. Zhong, Chitooligosaccharides prevents the development of colitis-associated colorectal cancer by modulating the intestinal microbiota and mycobiota, Front. Microbiol. 10 (2019) 2101, https://doi.org/10.3389/fmicb.2019.02101.
[49] L.Q. Zhu, L. Zhang, J. Zhang, G.L. Chang, G. Liu, D.-D. Yu, X.M. Yu, M.S. Zhao, B. Ye, Evodiamine inhibits high-fat diet-induced colitis-associated cancer in mice through regulating the gut microbiota, J. Integr. Med. 19 (2021) 56–65, https://doi.org/10.1016/j.joim.2020.11.001.
[50] B. Routy, E. Le Chatelier, L. Derosa, C.P.M. Duong, M.T. Alou, R. Daillère, A. Fluckiger, M. Messaoudene, C. Rauber, M.P. Roberti, M. Fidelle, C. Flament, V. Poirier-Colame, P. Opolon, C. Klein, K. Iribarren, L. Mondragón, N. Jacquelot, B. Qu, G. Ferrere, C. Clémenson, L. Mezquita, J.R. Masip, C. Naltet, S. Brosseau, C. Kaderbhai, C. Richard, H. Rizvi, F. Levenez, N. Galleron, B. Quinquis, N. Pons, B. Ryffel, V. Minard-Colin, P. Gonin, J.-C. Soria, E. Deutsch, Y. Loriot, F. Ghiringhelli, G. Zalcman, F. Goldwasser, B. Escudier, M.D. Hellmann, A. Eggermont, D. Raoult, L. Albiges, G. Kroemer, L. Zitvogel, Gut microbiome influences efficacy of PD-1-based immunotherapy against epithelial tumors, Science 359 (2018) 91–97, https://doi.org/10.1126/science.aan3706.
[51] M.I. Waly, A.S. Al-Rawahi, M. Al Riyami, M.A. Al-Kindi, H.K. Al-Issaei, S.A. Farooq, A. Al-Alawi, M.S. Rahman, Amelioration of azoxymethane induced-carcinogenesis by reducing oxidative stress in rat colon by natural extracts, BMC Complement. Alter. Med. 14 (2014) 60, https://doi.org/10.1186/1472-6882-14-60.
[52] W. Mao, Z. Zhu, Parthenolide inhibits hydrogen peroxide-induced osteoblast apoptosis, Mol. Med. Rep. 17 (2018) 8369–8376, https://doi.org/10.3892/mmr.2018.8908.

[53] D.V.T. da Silva, A.D. Pereira, G.T. Boaventura, R.S. de, A. Ribeiro, M.A. Verícimo, C.E. de Carvalho-Pinto, D. dos, S. Baião, E.M. Del Aguila, V.M.F. Paschoalin, Short-term betanin intake reduces oxidative stress in wistar rats, Nutrients 11 (2019) 1978, https://doi.org/10.3390/nu11091978.

[54] A.D. Waldman, J.M. Fritz, M.J. Lenardo, A guide to cancer immunotherapy: from T cell basic science to clinical practice, Nat. Rev. Immunol. 20 (2020) 651–668, https://doi.org/10.1038/s41577-020-0306-5.

[55] F. Grizzi, P. Bianchi, A. Malesci, L. Laghi, Prognostic value of innate and adaptive immunity in colorectal cancer, World J. Gastroenterol. 19 (2013) 174–184, https://doi.org/10.3748/wjg.v19.i2.174.

[56] E. Alemany-Cosme, E. Sáez-González, I. Moret, B. Mateos, M. Iborra, P. Nos, J. Sandoval, B. Beltrán, Oxidative stress in the pathogenesis of crohn's disease and the interconnection with immunological response, microbiota, external environmental factors, and epigenetics, Antioxidants 10 (2021) 64, https://doi.org/10.3390/antiox10010064.